Check for updates

Received: 22 January 2023 | Revised: 18 May 2023 | Accepted: 11 June 2023

DOI: 10.1111/jcpe.13843

ORIGINAL ARTICLE

Journal of Clinical Periodontology WILEY

Histological assessment and gene expression analysis of intra-oral soft tissue graft donor sites

Sandra Stuhr[1] | Felipe Nör[2] | Kareem Gayar[1] | Emilio Couso-Queiruga[1] | Leandro Chambrone[3,4,5] | Iñaki Gamborena[6,7,8] | Purnima Kumar[2] | Gustavo Avila-Ortiz[1] | Sukirth M. Ganesan[1]

[1]Department of Periodontics, University of Iowa College of Dentistry, Iowa City, Iowa, USA

[2]Department of Periodontics and Oral Medicine, University of Michigan School of Dentistry, Ann Arbor, Michigan, USA

[3]Evidence-Based Hub, Centro de Investigação Interdisciplinar Egas Moniz (CiiEM), Egas Moniz, CRL, Monte de Caparica, Portugal

[4]Unit of Basic Oral Investigations (UIBO), School of Dentistry, Universidad El Bosque, Bogotá, Colombia

[5]Department of Periodontics, School of Dental Medicine, The University of Pennsylvania, Philadelphia, Pennsylvania, USA

[6]Private Practice, San Sebastian, Spain

[7]Department of Preventive and Restorative Sciences, University of Pennsylvania School of Dental Medicine, Philadelphia, Pennsylvania, USA

[8]Department of Restorative Dentistry, University of Washington School of Dentistry, Seattle, Washington, USA

Correspondence
Gustavo Avila-Ortiz, Private practice, Atelier Dental Madrid, C/ Blanca de Navarra 10, Madrid 28003, Spain; Department of Oral Medicine, Infection, and Immunity, Division of Periodontology, Harvard School of Dental Medicine, 188 Longwood Ave, Boston, MA 02115, USA.
Email: gustavo_avila-ortiz@hsdm.harvard.edu

Sukirth M. Ganesan, Department of Periodontics, University of Iowa College of Dentistry, 801 Newton Road, Iowa City, IA 52242, USA.
Email: sukirth-ganesan@uiowa.edu

Present addresses
Sandra Stuhr, Department of Periodontics and Oral Medicine, University of Michigan School of Dentistry, Ann Arbor, Michigan, USA; Emilio Couso-Queiruga, Department of Oral Surgery and Stomatology, University of Bern School of Dental Medicine, Bern, Switzerland; Gustavo Avila-Ortiz, Private Practice, Atelier Dental Madrid, Spain; and Department of Oral Medicine, Infection, and Immunity, Harvard School of Dental Medicine, Boston, Massachusetts, USA.

Funding information
University of Iowa

Abstract

Aim: To determine the structural and gene expression features of different intra-oral soft tissue donor sites (i.e., anterior palate, posterior palate, maxillary tuberosity and retromolar pad).

Materials and Methods: Standardized mucosal tissue punch biopsies were collected from at least one donor site per subject. Histological processing was performed to determine tissue morphometry and quantify collagen composition. Site-specific gene distribution was mapped using targeted gene expression analysis and validated using real time polymerase chain reaction (qPCR).

Results: A total of 50 samples from 37 subjects were harvested. Epithelial thickness did not differ between sites. However, lamina propria was thicker in the maxillary tuberosity (2.55 ± 0.92 mm) and retromolar pad (1.98 ± 0.71 mm) than in the lateral palate. Type I collagen was the predominant structural protein in the lamina propria (75.06%–80.21%). Genes involving collagen maturation and extracellular matrix regulation were highly expressed in the maxillary tuberosity and retromolar pad, while lipogenesis-associated genes were markedly expressed in the lateral palate. The retromolar pad showed the most distinct gene expression profile, and the anterior and posterior palate displayed similar transcription profiles.

Conclusions: Tissue samples harvested from the anterior and posterior palate differed morphologically from those from the maxillary tuberosity and retromolar pad.

This is an open access article under the terms of the Creative Commons Attribution-NonCommercial-NoDerivs License, which permits use and distribution in any medium, provided the original work is properly cited, the use is non-commercial and no modifications or adaptations are made.
© 2023 The Authors. *Journal of Clinical Periodontology* published by John Wiley & Sons Ltd.

Each intra-oral site showed a unique gene expression profile, which might impact their biological behaviour and outcomes of soft tissue augmentation procedures.

KEYWORDS

connective tissue, gene expression, histology, oral mucosa, phenotype

Clinical Relevance

Scientific rationale for study: Autologous soft tissue grafts are routinely used in periodontal and implant-related plastic surgery. However, evidence is scarce regarding the specific biological properties of tissues obtained from different intra-oral donor sites.

Principal findings: Although epithelial thickness was similar between donor sites, lamina propria was thicker in maxillary tuberosity and retromolar pad compared to palatal samples. A higher percentage of collagen type I than collagen type III was observed in all groups. Genes related to distinct cellular functions, such as collagen biosynthesis, extracellular matrix organization and cell signalling, varied in expression depending on the donor site.

Practical implications: Donor tissue harvested from the anterior and posterior palatal regions showed distinct structural and genetic differences compared to the maxillary tuberosity and retromolar pad. Knowledge on gene expression profiles may be used for clinical decision making regarding the choice of donor site and expected healing outcomes after soft tissue augmentation.

1 | INTRODUCTION

Soft tissue augmentation procedures aimed at periodontal and peri-implant phenotype modification have evolved over the past several decades (Avila-Ortiz et al., 2022; Chambrone et al., 2018; Chambrone & Ortiz, 2022). Autologous subepithelial connective tissue graft (SCTG) is currently considered the gold standard for soft tissue augmentation in periodontal plastic surgery involving natural teeth, edentulous sites and dental implants due to its high predictability and effectiveness (Barootchi et al., 2020; Cairo et al., 2014; Chambrone et al., 2008; Tavelli et al., 2021). However, the quantity of available SCTG is limited by the site of harvest and intrinsic anatomical differences among patients (Del Pizzo et al., 2002; Griffin et al., 2006). Although SCTGs are commonly harvested from the palatal region because of accessibility and typically larger dimensions, other locations (e.g., maxillary tuberosity [MT]) may serve as donor sites (Gamborena & Markus, 2014; Meltzer, 1979). Currently, the choice of the donor site is generally based on the clinician's preference, as differences in biological properties and outcomes based on harvest site are still unclear (Zuhr et al., 2014).

The characteristics of the donor site might influence post-operative healing and surgical outcomes. For example, it has been suggested that SCTGs from the tuberosity may have less post-operative shrinkage, as they contain more collagen and less adipose tissue compared with those from the anterior palate (AP) (Zuhr et al., 2014). Even within SCTGs harvested from the palate, variations in the proportions of adipose tissue and lamina propria have been observed (Harris, 2003). Other studies have noted differences in collagen cross-linking and maturation between SCTGs obtained from the palate and the tuberosity (Dellavia et al., 2014; Kagan, 1986). More recently Sanz-Martin et al. (2019) found a greater percentage of lamina propria and a lower percentage of submucosa in the tuberosity region than in the palate.

The expected healing response and the associated patient morbidity also may play a role in the selection of the SCTG donor site. Interestingly, epithelial cells from the hard palate have been shown to harbour unique proliferative heterogeneity due to the influence of various factors on stem cell activity, such as specific location and masticatory activity (Byrd et al., 2019).

Differences in tissue macrostructure and the biological activity of individual cell types may vary between specific intra-oral sites and could have an impact on clinical outcomes. However, there is limited comprehensive information on structural features and gene expression profiles of SCTGs from different intra-oral locations. Therefore, this study aimed to analyse the histological characteristics and the gene expression profiles of sub-epithelial connective tissue samples (SCTS) collected from four different intra-oral locations: AP, posterior palate (PP), MT and retromolar pad (RP).

2 | MATERIALS AND METHODS

2.1 | Experimental design and centre

This cross-sectional clinical study was conducted in the Department of Periodontics, University of Iowa College of Dentistry and Dental Clinics, between November 2020 and May 2021 in compliance with Strengthening the Reporting of Observational Studies in Epidemiology (STROBE) guidelines for cross-sectional studies (von Elm et al., 2007).

1600051x, 2023, 10, Downloaded from https://onlinelibrary.wiley.com/doi/10.1111/jcpe.13843 by Schweizerische Akademie Der, Wiley Online Library on [16/09/2023]. See the Terms and Conditions (https://onlinelibrary.wiley.com/terms-and-conditions) on Wiley Online Library for rules of use; OA articles are governed by the applicable Creative Commons License

2.2 | Ethical approval and registration

Approval for the experimental protocol was obtained from the University of Iowa Institutional Review Board in November 2020 (HawkIRB #202006325).

2.3 | Outcomes of interest

Histomorphometric outcomes

- Epithelium and lamina propria thickness.
- Relative percentages of collagen types I and III (COL-I and COL-III) in the lamina propria.

Gene expression outcomes

- Quantification of gene expression related to soft tissue differentiation, proliferation, angiogenesis, inflammation and potential for maturation at each site.

2.4 | Eligibility criteria and recruitment

The inclusion criterion was as follows: systemically healthy (American Society of Anesthesiology I/II) adults (≥18 years of age) who required surgical procedures or sub-epithelial connective tissue graft harvesting in one of the regions of interest.

The exclusion criteria were as follows: (1) current or heavy smokers, defined as subjects who have smoked >10 cigarettes per day within 6 months of study onset and have smoked >100 cigarettes in their lifetime; (2) uncontrolled diabetes mellitus (defined as HbA1c > 7.0%); (3) liver or kidney failure; (4) active local or systemic infections; (5) current chemo- or radiotherapy or history of radiotherapy in the head and neck area in the last 18 months; (6) severe haematological disorders; (7) any autoimmune disorder, inflammatory condition or medications that may compromise normal wound healing; (8) pregnant or nursing women; (9) removable prosthesis resting in the sites of interest and (10) unwilling or unable to sign the informed consent.

2.5 | Clinical procedures

All surgical procedures were performed under local anaesthesia. A uniform full-thickness mucosal sample was obtained by means of a standardized 4-mm tissue punch (Integra Miltex, Integra LifeSciences, Princeton, NJ, USA) as illustrated in Figure 1. All harvesting procedures were completed by supervised residents and/or faculty members in the Department of Periodontics, University of Iowa. All samples were harvested at a safe distance from the gingival margin of adjacent teeth to prevent the occurrence of clinical attachment loss. Four regions of interest were defined as follows (Figure 2):

- AP: the region from the mesial of the maxillary lateral incisor to the distal of the maxillary first premolar;
- PP: the region from the mesial of the maxillary second premolar to the distal of the maxillary second molar, if present;
- MT: the anatomical region distal to the most posterior maxillary tooth, up to the first molar;
- RP: the anatomical region distal to the most posterior mandibular tooth, up to the first molar.

After harvesting, the samples were bisected, and one portion was stored in a 10% buffered formalin solution for histological analysis. The remaining portion was then divided in half, with one portion being stored in 1 mL RNALater stabilization solution (Thermo Scientific, USA) and the other frozen at −20°C for gene expression and real-time polymerase chain reaction (RT-PCR) analysis. The formalin-fixed samples were submitted to the University of Iowa, Department of Oral Pathology Core, for paraffin embedding. Samples were assigned a code based on the donor site. Up to four samples could be collected per subject, with a maximum of one sample per site if the surgery encompassed multiple regions of interest.

2.6 | Histological analysis

All formalin-fixed tissue samples were used for histological analysis. The previously bisected samples were embedded in paraffin on their cut surface and serial histological sections (4-μm thickness) were made by one independent examiner (SS). Haematoxylin and eosin (H&E) and Picrosirius red staining (PRS) were used to visualize different tissue characteristics. H&E staining was performed using an automated system in one run to prevent batch effects in the staining process (Sakura Tissue-Tek DRS 2000, USA). PRS was performed by two trained individuals (SS and KG) according to manufacturer's instructions (NovaUltra, USA). Finally, sections were mounted in a resinous medium (Epredia, Fisher Scientific). All stained slides were reviewed by a board-certified oral pathologist (FN) to confirm appropriate sectioning, staining and embedding/orientation. Cases showing tangential sectioning or absent epithelium were excluded from the linear measurements, after several attempts to reorient the specimen in the paraffin block. Samples that were compromised because of processing errors were excluded from linear measurements. The PRS sections were examined under normal and polarized light, the latter images using a light microscope (Olympus LS BX53, Japan). Photomicrographs were obtained at a constant magnification (40×) for collagen quantification and at 20× for linear measurements of structural components by an independent examiner (GAO) using a light microscope (Zeiss Primo Star, Germany). A duplicate copy of each sample was labelled with computer-generated, randomized numeric digits (String Generator, Random.org). Representative sections of each area of harvest are shown in Figure 3.

All histomorphometric assessments were made by two independent examiners (SS and FN) who were calibrated on 10 unrelated tissue sections. Linear measurements of epithelial, lamina propria and

1600051x, 2023, 10, Downloaded from https://onlinelibrary.wiley.com/doi/10.1111/jcpe.13843 by Schweizerische Akademie Der, Wiley Online Library on [16/09/2023]. See the Terms and Conditions (https://onlinelibrary.wiley.com/terms-and-conditions) on Wiley Online Library for rules of use; OA articles are governed by the applicable Creative Commons License

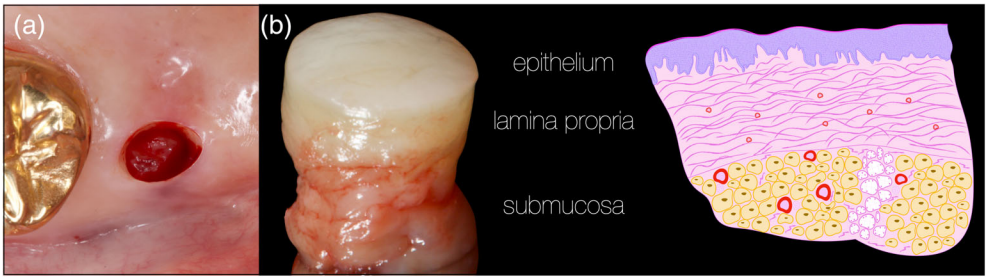

FIGURE 1 Representative clinical image and illustration of a sample harvested as part of this study. (a) Donor site, in this case maxillary tuberosity region, after tissue sample collection. (b) Main layers of the tissue sample, prior to bisection, from superficial to deep: epithelium, lamina propria and submucosa.

FIGURE 2 Visual depiction of the pre-defined anatomical locations where samples were harvested: anterior palate (green), posterior palate (yellow), maxillary tuberosity (blue) and retromolar pad (orange).

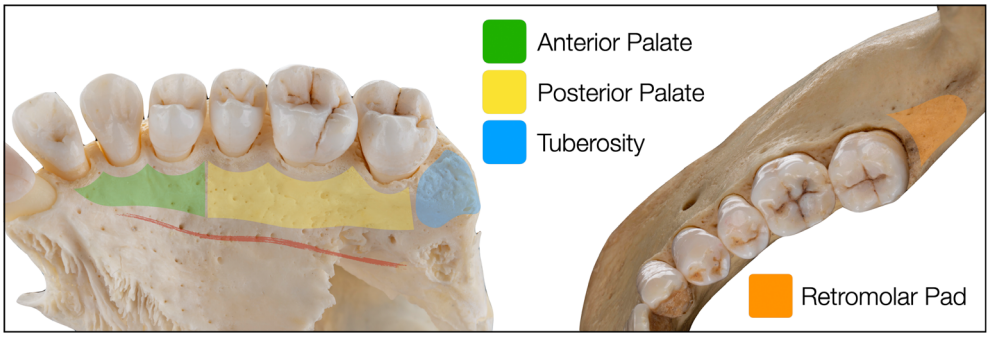

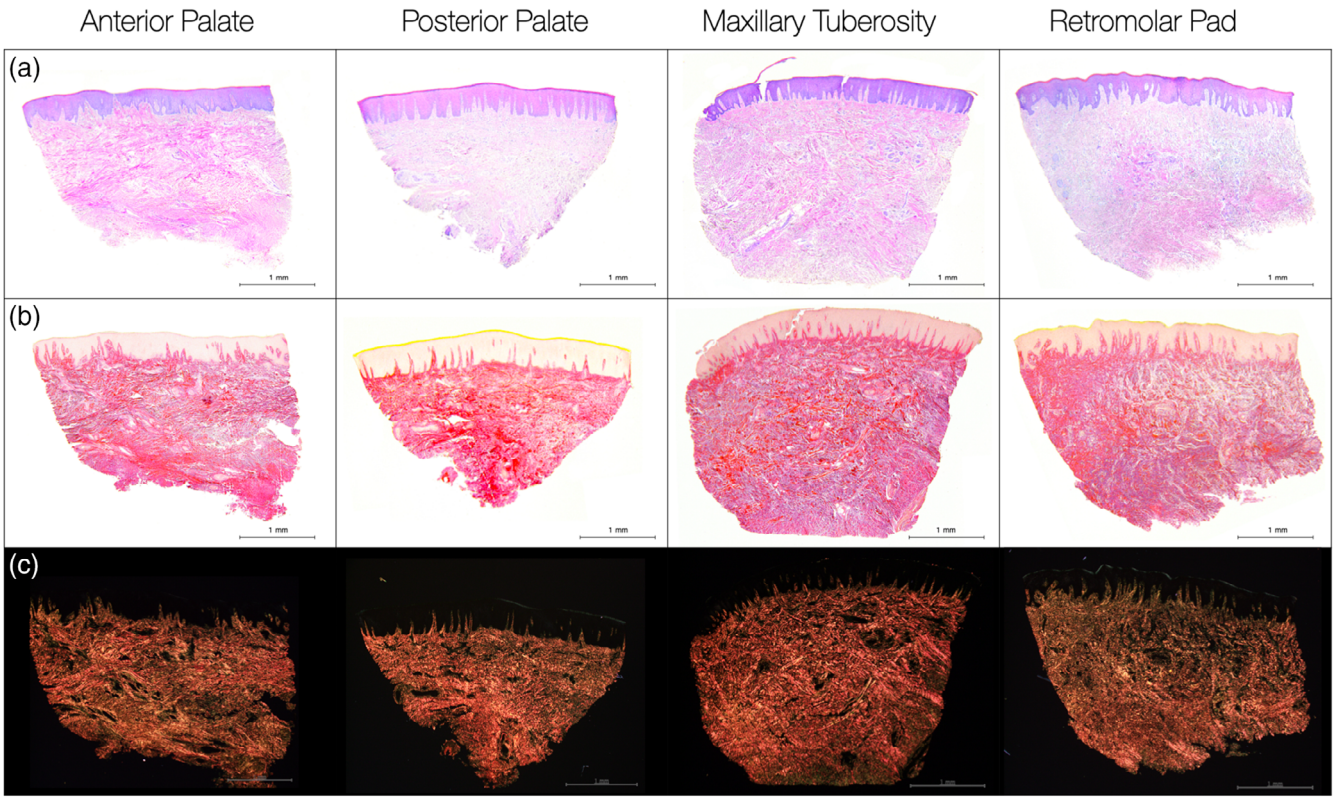

FIGURE 3 Photomicrographs of representative tissue samples from each donor site. (a) Haematoxylin and eosin staining. (b) Picrosirius red staining. (c) Polarized images from the Picrosirius red stained slides.

1600051x, 2023, 10, Downloaded from https://onlinelibrary.wiley.com/doi/10.1111/jcpe.13843 by Schweizerische Akademie Der, Wiley Online Library on [16/09/2023]. See the Terms and Conditions (https://onlinelibrary.wiley.com/terms-and-conditions) on Wiley Online Library for rules of use; OA articles are governed by the applicable Creative Commons License

submucosa thickness were performed in triplicate and averaged. Each section had a pre-established horizontal line delineating the lamina propria from the submucosa layer, if present. If the submucosa layer was not present, a horizontal line at the base of the tissue specimen was pre-established by a board-certified oral pathologist (FN) prior to subsequent measurements. The first vertical measurement was made at the tissue section's midpoint to divide the specimen into two equal halves, and then each half was subsequently measured lengthwise at its midpoint. Tukey honestly significant difference (HSD) was used to determine the statistical significance in epithelial and lamina propria thickness between the various donor sites.

PRS sections were analysed under polarized light for collagen quantification. COL-I fibres were stained in red, and COL-III fibres were stained in green. Quantitative analysis was performed using the software package ImageJ (National Institutes of Health, Bethesda, MD, USA) using the Red/Green/Blue profiling tool, which gave an estimate of the relative proportions. Tukey HSD was used to determine the statistical significance in collagen proportions between the various donor sites.

2.7 | Gene expression analysis

RNA isolation was achieved using the QIAGEN AllPrepDNA/RNA FFPE kit. The isolated RNA was hybridized with reporter and capture probes for a human fibrosis panel and nCounter analysis (nanoString Technologies, USA). The human fibrosis panel profiled 770 genes across 51 annotated pathways involving immune responses to tissue damage, inflammation, proliferation, extracellular matrix modifications and tissue alterations. Transcript counts less than the mean of the negative controls (±1 SD) were considered as background and excluded. Quantitative data were normalized to house-keeping genes, analysed and visualized using volcano plots using the nCounter analysis platform (nSolver 4.0 Analysis Software, R 3.3.2, and the Advanced Analysis 2.0 plugin, nanoString Technologies, USA). Findings from the nCounter analysis were validated using RT-PCR.

2.8 | Real-time polymerase chain reaction

The top nine of the most differentially expressed genes and those genes that contributed to the critical function in the tissue were derived from the targeted RNA profiling analysis and analysed using RT-PCR (*ACACA*, *CXCL12*, *ERO1A*, *GATA3*, *KLRD1*, *SERPINF1*, *THBS2*, *COL1A1* and *COL3A1*). The selected genes related to collagen biosynthesis (*COL1A1*, *COL3A1* and *THBS2*), extracellular matrix synthesis (*SERPINF1*), lipogenesis (*ACACA*), focal adhesion signalling (*GATA3*) and cell signalling (*CXCL12*, *ERO1A* and *KLRD1*).

Total RNA was isolated using the RNeasy Mini Kit according to manufacturer's instructions (Qiagen, USA). RNA concentration was calculated using the NanoDrop 1000TM spectrophotometer (Thermo Scientific, USA). Primers were selected based on applications previously reported in peer-reviewed, published human studies (Table S1). PCR initial activation was performed. Reverse transcription was completed with total RNA using the First Strand cDNA Synthesis Kit (Syd Labs, USA). After RT reaction was performed, the resulting first-strand cDNA was used for real-time PCR analysis in an Agilent MX3005P instrument. *HPRT1* was used as the house-keeping gene for normalization, and assay was performed in triplicates. Fold changes were calculated by comparing the normalized cycle threshold (Ct) values from different sites to the PP site.

2.9 | Sample size calculation

The sample size calculation of this study was based on the mean values of previous studies where the density of collagen in samples obtained from the tuberosity and palate was compared (Bertl et al., 2015; Dellavia et al., 2014). The minimum sample size of 11 per group resulted from a power analysis calculation, considering the number of groups (4), a power of 0.8, effect size of 0.7 and a significance level of at least 0.05 (G*Power, version 3.1).

3 | RESULTS

3.1 | Demographic characteristics

A total of 50 samples from 37 patients who fulfilled the inclusion and exclusion criteria were included in this study. The study population comprised 64.9% females and 35.1% males, and the mean age was 46.4 ± 15 (range: 19–77). All patients were non-smokers. Three patients had well-controlled type II diabetes (1 PP and 2 RP). Baseline demographic data per group are shown in Table 1. No significant differences were observed between the groups.

3.2 | Sample characteristics

Thirteen AP, 13 PP, 12 MT and 12 RP SCTS were collected. Two PP and RP samples were excluded from linear measurement analysis and one RP sample was excluded from the collagen quantification because of embedding error or processing distortion. Two PP samples were also excluded from gene expression analysis because of inadequate RNA counts, leading to a total of 11 samples in the PP group.

3.3 | Histological and histomorphometric analyses

Specimens from AP, PP, MT and RP were surfaced by orthokeratinized stratified squamous epithelium with a prominent granular layer featuring well-defined, uniformly long epithelial rete ridges. This pattern of keratinization and the presence of demarcated rete ridges are features commonly seen in the oral epithelium that is attached to underlying bone (i.e., attached mucosa), which corresponds to the anatomical location of the specimens. The mean epithelial thickness

1600051x, 2023, 10, Downloaded from https://onlinelibrary.wiley.com/doi/10.1111/jcpe.13843 by Schweizerische Akademie Der, Wiley Online Library on [16/09/2023]. See the Terms and Conditions (https://onlinelibrary.wiley.com/terms-and-conditions) on Wiley Online Library for rules of use; OA articles are governed by the applicable Creative Commons License

TABLE 1 Demographic and clinical data.

Parameters	Anterior palate	Posterior palate	Maxillary tuberosity	Retromolar pad
Number of samples	13	13	12	12
Gender				
Males (*n*, %)	5, 38.5	3, 23.1	6, 50.0	5, 42.7
Females (*n*, %)	8, 61.5	10, 76.9	6, 50.0	7, 58.3
Age (years)	40.6	46.6	54.5	49.8
Race				
African American/Black (*n*, %)	2, 15.4	1, 7.7	1, 8.3	2, 16.7
Asian (*n*, %)	1, 7.7	-	-	2, 16.7
Caucasian/White (*n*, %)	10, 76.9	12, 92.3	11, 91.7	8, 66.6
Ethnicity				
Hispanic or Latino (*n*, %)	3	2	2	1
Not Hispanic or Latino (*n*, %)	10	11	10	11
Diabetics (*n*)	-	1	-	2
HbA1c (mean %)	-	5.3	-	6.95
Smokers (*n*)	-	-	-	-

TABLE 2 Vertical linear measurements (average in millimetres ± standard deviation) and collagen I and III proportions (%).

Parameters	Anterior palate	Posterior palate	Maxillary tuberosity	Retromolar pad
Epithelial thickness (mm)	0.47 ± 0.06	0.41 ± 0.06	0.45 ± 0.10	0.48 ± 0.15
Lamina propria thickness (mm)	0.92 ± 0.35	1.18 ± 0.37	2.55 ± 0.92	1.98 ± 0.71
COL-I (%)	75.22 ± 5.1	76.1 ± 9.11	80.21 ± 9.26	75.06 ± 5.41
COL-III (%)	4.2 ± 2.6	6.49 ± 5.97	2.99 ± 1.60	2.1 ± 1.83

Abbreviations: COL-I, collagen type I; COL-III, collagen type III.

was 0.47 ± 0.06 mm for AP ($n = 13$), 0.41 ± 0.06 mm for PP ($n = 11$), 0.45 ± 0.10 mm for MT ($n = 12$) and 0.48 ± 0.15 mm for RP ($n = 10$), as shown in Table 2 (Tukey HSD, $p > .05$). Although not statistically significant, a subset of cases from MT and RP showed a slightly thicker epithelial layer with associated areas of hyperkeratosis compared to AP and PP, which may be explained by a greater exposure of MT and RP sites to trauma, especially during mastication. Importantly, no epithelial atypia or dysplasia was identified (Figure S1A1–D1).

The underlying lamina propria showed variability in thickness across the samples. The mean lamina propria thickness was 0.92 ± 0.35 mm for AP, 1.18 ± 0.37 mm for PP, 2.55 ± 0.92 mm for MT and 1.98 ± 0.71 mm for RP (Table 2). The lamina propria was significantly thicker in MT and RP (Tukey HSD, $p < .05$) compared to AP and PP sites, as shown in Table 3. The overall intra-class correlation coefficient (ICC) for linear measurements was 0.91 (95% CI: 0.842–0.949). In regard to density, collagen fibres were more loosely arranged in AP and PP sites with H&E stain, whereas a denser arrangement of collagen fibres was observed in MT and RP sites (Figure S1A1–D1). To further explore these findings, PRS was performed to determine the presence and distribution pattern of COL-I and COL-III. The ICC was 0.88 (95% CI: 0.796–0.932). An overall higher percentage of COL-I than COL-III (Table 2) was observed in all groups. An additional bar graph representing the collagen I and III distribution is available as Figure S2. AP samples had 75.22 ± 5.1% COL-I and 4.2 ± 2.6% COL-III. PP samples showed 76.1 ± 9.11% COL-I and 6.49 ± 5.97% COL-III. MT sites showed 80.21 ± 9.26% COL-I and 2.99 ± 1.60% COL-III. RP sites contained 75.06 ± 5.41% COL-I and 2.1% ± 1.83% COL-III (Table 2). RP samples had significantly lower amounts of COL-III compared to AP and PP ($p < .05$), as shown in Table 3. However, based on a visual analysis and in congruence with the data from H&E stained samples, the collagen bundles, especially COL-1, appeared to be thickest in this group (Figure S1D3). The percentage of COL-1 was also higher in MT, which also correlates with the denser arrangement of collagen fibres previously observed on H&E-stained slides from this group. Remarkably, the staining pattern of COL-1 appeared to be more homogeneously distributed across the samples from the MT group compared to the other sites (Figure S1C3). The highest concentration of COL-III was seen in the PP group, which also showed an apparent predilection of COL-III for the upper portions of the lamina propria, in close proximity to the surface epithelium (Figure S1B3). Representative highly magnified histological images of each donor site are shown in Figure S3. The presence and distribution of blood vessels, nerve fibres and chronic inflammatory infiltrates were within the normal limits in all groups.

1600051x, 2023, 10, Downloaded from https://onlinelibrary.wiley.com/doi/10.1111/jcpe.13843 by Schweizerische Akademie Der, Wiley Online Library on [16/09/2023]. See the Terms and Conditions (https://onlinelibrary.wiley.com/terms-and-conditions) on Wiley Online Library for rules of use; OA articles are governed by the applicable Creative Commons License

TABLE 3 Vertical linear lamina propria measurements and collagen I/III inter-group comparisons.

Parameter	Donor site 1	Donor site 2	*p*-Value (Tukey HSD)
LP thickness (mm)	PP	AP	.763
LP thickness (mm)	MT	AP	1.52E-06*
LP thickness (mm)	RP	AP	.002*
LP thickness (mm)	MT	PP	7.96E-05*
LP thickness (mm)	RP	PP	.041*
LP thickness (mm)	MT	RP	.211
%COL-1	MT	AP	.242
%COL-1	MT	PP	.289
%COL-1	MT	RP	.281
%COL-1	PP	AP	.505
%COL-1	RP	AP	.817
%COL-1	RP	PP	.451
%COL-3	MT	RP	.132
%COL-3	PP	AP	.330
%COL-3	MT	AP	.568
%COL-3	MT	PP	.183
%COL-3	RP	AP	.049*
%COL-3	RP	PP	.049*

Abbreviations: AP, anterior palate; COL-I, collagen type I; COL-III, collagen type III; HSD, honestly significant difference; LP, lamina propria; MT, maxillary tuberosity; PP, posterior palate; RP, retromolar pad.
*$p < .05$.

3.4 | Gene expression analyses

The panel included 770 genes associated with 51 pathways and functions. A total of 523 genes were identified in our samples for comparative analyses based on the threshold values (as described in Section 2.7). Because the palate is the most used donor site, we first compared PP and AP. Our analysis showed that gene expression profiles were not significantly different between AP and PP sites (Benjamini–Yekutieli adjusted $p > .05$) (Table S2). However, when AP and PP sites were compared to other donor sites, gene expression differed significantly. Differences in major gene functions and interactions between donor sites are presented in Figure 4a, along with gene Venn diagrams showing the overlap among relevant genes in Figure 4b,c.

Overall, genes belonging to collagen biosynthesis (*COL1A1*, *COL3A1*, *COL6A3*, *COL16A1*, *PPARGC1A* and *THBS2*), extracellular matrix synthesis (*ACTA2* and *SERPINF1*), lipogenesis (*ACACA*, *ELOVL6* and *PNPLA3*), coagulation (*PROS1* and *THBS2*), focal adhesion signalling (*ATP7A* and *GATA3*) and cell signalling (*CXCL12*, *IL1R1*, *KLRD1*, *DUSP8*, *ERN1*, *ERO1A*, *FCER1G* and *VAMP8*) differed significantly between donor sites ($p < .05$). RP sites showed the most differentially abundant genes. Compared to PP sites, MT sites exhibited significantly lower expression of the lipogenesis-associated *ACACA* (Benjamini–Yekutieli adjusted $p < .05$), and RP sites exhibited several significantly overexpressed and underexpressed genes, with the most differentially expressed $\log_2$ 2-fold change related to signalling-associated genes. A full list of specific *p*-values for each gene comparison is shown in Table S2 and volcano plots in Figure S4.

Data analyses on the final set of nine differentially expressed genes showed at least a twofold change average, relative to PP, in five genes related to collagen biosynthesis and cell signalling: *COL1A1* (MT and RP), *CXCL12* (MT), *ERO1A* (RP), *GATA3* (RP and MT) and *THBS2* (MT, RP and AP). Changes in the fold change are shown in Figure S5. Raw PCR data for each group are shown in Table S3.

Additionally, relative abundances of genes within each donor site were calculated. Individual relative abundances of genes within the group and median abundances per group are shown in Table S4. Genes contributing to 25% of the total gene expression profiles within each donor site are also reported. Overall, the top 25% of genes highly expressed and shared between all groups included *FABP5*, *RPS27A*, *VIM* and *COL3A1* (Figure 4b). Interestingly, *COL1A1* and *COL1A2* were not expressed in the top 25% of the AP group in terms of relative abundance. Additionally, the AP group showed a higher relative abundance of the angiogenesis-related marker Complement Factor H (*CFH*) (0.75% of total gene abundance and ranked 15 out of 760 genes in terms of relative abundance) compared to PP (0.34%, ranked 52/760), MT (0.38%, ranked 42/760) and RP (ranked 66/760). *S100A4*, an indirect participant in angiogenesis, was more abundant in the MT (0.69%) and RP (0.60%) groups (ranked 14 and 18, out of 760, respectively) compared to the AP (0.52%, 33/760) and PP (0.48%, 34/760) groups. A gene expression database of relevant markers referenced in this study is included in Table S5.

1600051x, 2023, 10, Downloaded from https://onlinelibrary.wiley.com/doi/10.1111/jcpe.13843 by Schweizerische Akademie Der, Wiley Online Library on [16/09/2023]. See the Terms and Conditions (https://onlinelibrary.wiley.com/terms-and-conditions) on Wiley Online Library for rules of use; OA articles are governed by the applicable Creative Commons License

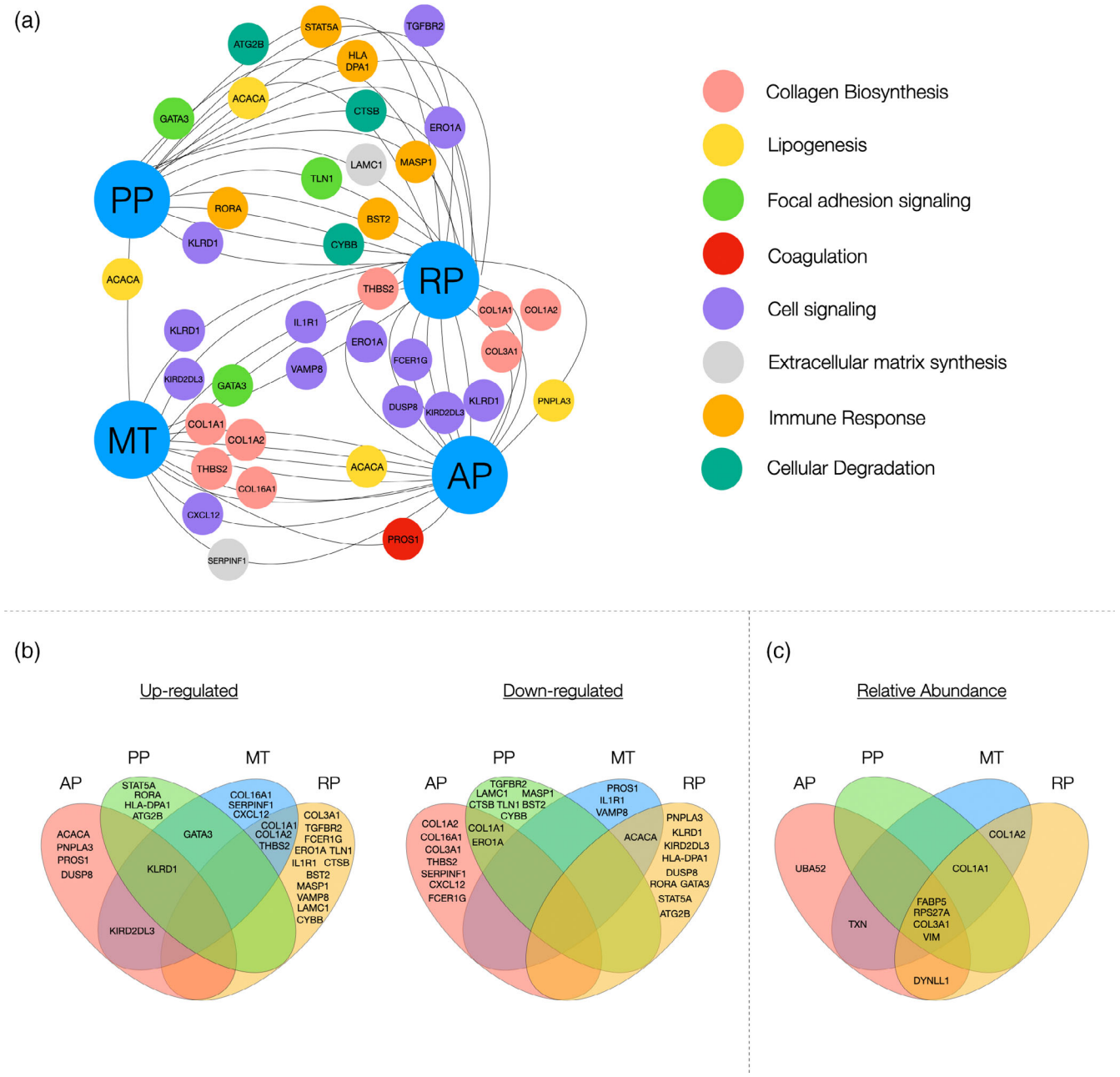

FIGURE 4 (a) Illustration showing genes that were statistically significantly overexpresssed or underexpressed in comparative analyses. Genes closer to the donor site acronym (labelled in blue) were more highly expressed, and genes that are farther away were underexpressed compared to the opposing donor site. Proximity of the labelled gene to each donor site was based on fold-change differences, that is, the closer to the site, the higher the fold-change difference. Colour coding is based on major gene functions relative to this study. (b) Gene Venn diagrams showing the overlap of genes within each inter-group comparison. Each gene displayed here was significantly overexpressed or underexpressed in a direct gene comparison with the other three groups. (c) Gene Venn diagram based on the relative abundance of the expressed genes in each group. The top 25% most abundant genes that are distinct in each of the sites are displayed. AP, anterior palate; MT, maxillary tuberosity; PP, posterior palate; RP, retromolar pad.

4 | DISCUSSION

Our findings show that structural and genetic differences exist between different intra-oral donor sites for SCTG, with MT and RP sites exhibiting, on average, 1.5–2 times greater lamina propria thickness relative to the lateral palate. The thicker lamina propria in MT and RP sites may yield a thicker and denser SCTG when augmentation of a larger contour deficiency is required, particularly in situations when increased keratinized tissue width and mucosal thickness are desired (Tavelli et al., 2019). Evaluation of the collagen content showed an overall higher proportion of COL-I compared to COL-III in all groups. These findings are in accordance with a previous study

1600051x, 2023, 10, Downloaded from https://onlinelibrary.wiley.com/doi/10.1111/jcpe.13843 by Schweizerische Akademie Der, Wiley Online Library on [16/09/2023]. See the Terms and Conditions (https://onlinelibrary.wiley.com/terms-and-conditions) on Wiley Online Library for rules of use; OA articles are governed by the applicable Creative Commons License

comparing collagen content of the tuberosity to the palate (Dellavia et al., 2014). In addition, our data identified approximately a fivefold and threefold increase in the COL1A1 expression in MT and RP areas compared to the palate, respectively. This increase in *COL1A1* gene is likely related to the observed COL-1 proportions in the histological assessment.

Several studies have reported excellent dimensional stability and even a hyperplastic response over time in sites augmented with tuberosity SCTG (Dellavia et al., 2014; Gamborena & Markus, 2014; Gluckman et al., 2019; Jung et al., 2008). It has been hypothesized that this hyperplastic response is related to enzymatic activity of lysyl hydroxylase (LH) and its role in collagen maturation via post-translational hydroxylation, specifically its predominant form LH2b, given its overexpression in fibrotic processes (van der Slot et al., 2004; Walker et al., 2005). In the tuberosity, it has also been hypothesized that collagen could exhibit a higher level of cross-linking, leading to less degradation by matrix metalloproteinases and lower post-surgical remodelling (Kagan, 1986). Although our study did not assess LH2b, thrombospondins were evaluated for their role in regulating proteins that work concertedly with LH in collagen cross-linking. Specifically, *THBS2* regulates lysyl oxidase, which then works in unison with LH in collagen cross-linking. It is hypothesized that overhydroxylation of these lysyl residues may play a major role in fibrosis (Kamel et al., 2017). Remarkably, we observed a 7.2-fold change in overexpression of *THBS2* in the MT compared to PP. Critically, LH has been studied as the primary target for *GATA3*, and we were able to identify approximately a 12-fold increase in *GATA3* in the tuberosity compared to the palate. Thus, LH-dependent collagen maturation is predominant in MT sites compared to PP sites (Liu et al., 2018). Furthermore, although *GATA3* plays an active role in inflammation, it also participates in tissue fibrosis. Recent studies have evaluated *GATA3*'s role as a regulator of macrophage diversification, suggesting that *GATA3*-positive macrophages display an M2 polarized phenotype (Yang et al., 2018). In addition, overexpression of *GATA3* has been associated with a fibrotic phenotype in cardiac tissue.

Limited evidence indicates that biological features of subepithelial connective tissue (SCT), which appear to be directly related to the origin of the graft, may influence the outcomes of surgical therapy. Within our knowledge, this study is the first to explore the biological underpinnings contributing to phenotypic heterogeneity and different proliferative properties of SCT of intra-oral origin in four different donor sites. An increase in the multi-fold expression of *COL1A1*, *THBS2* and *GATA3* in the tuberosity and RP regions may explain the clinically observed thicker and denser SCTGs compared to the PP. In addition, tuberosity sites also exhibit a significantly lower expression of non-collagen-related genes, such as lipogenesis-associated acetyl Co-A carboxylase alpha (*ACACA*), potentially contributing to the observed thicker phenotype (Collins et al., 2011). Along with lipogenesis-related markers, genes related to angiogenesis (*CFH*) and coagulation (*PROS1*) were more abundant in the AP group compared to all other groups. *CFH* is a regulator of the complement system, and may impact angiogenic pathways (Liu & Hoh, 2017).

Intriguingly, although both the retromolar and tuberosity regions exhibited denser and thicker SCTGs, our study identified distinct underlying genetic drivers. For example, only the retromolar site showed a sevenfold increase in endoplasmic reticulum oxidase 1α (*ERO1A*). Loss of function of *ERO1A* has been shown to interfere with pro-collagen intracellular maturation and compromised extracellular matrix (Zito et al., 2012). Therefore, in addition to the LH-dependent collagen maturation and *COL1A1* overexpression, *ERO1A* may also contribute to the observed thicker and denser lamina propria phenotype in RP sites.

RP also exhibited higher expression of *IL1R1* than MT. This may be attributable to the constitutive immune surveillance phenomenon involving regulation of the individual's overall immune status, which is influenced by the inflammatory response to different stimuli and activity of oral mucosal epithelial cells (Perrier et al., 2002; Smith et al., 2005). Alternatively, although an attempt was made to harvest samples away from the mucosal margin, access to the retromolar region is often challenging, which may have led to unintentional collection of marginal tissue with subclinical inflammation that may explain the higher expression of *IL1R1* in RP samples.

Greater expression of *CXCL12* was also observed, most significantly in the MT group compared to the PP group. *CXCL12* is basally expressed in both haematopoietic and non-haematopoietic tissue, including the mucosal epithelium, and has been shown to be up-regulated in response to tissue damage, chronic immune activation, pre-malignant lesions and tumour cell metastasis (Wang et al., 2009; Xia et al., 2012). In these destructive situations, one of *CXCL12*'s receptors, *CXCR4*, is typically found to be up-regulated as well. However, our data did not support up-regulation of *CXCR4*, suggesting that the biological activity of *CXCL12*, although identified because of lack of the receptor, is probably minimal or null in clinically healthy tissue samples.

This study is not exempt from limitations. Although the SCTS were not labelled with identifiers during the measurements, one of the examiners completed the sectioning, so it was not possible to be truly blinded for the histomorphometric measurements. This was compensated by the addition of another calibrated, blinded examiner who was not aware of the SCTS donor site. It should also be considered that structural and gene expression features of the oral tissues may be affected by environmental factors such as the patient's diet and parafunctional habits. Inter- and intra-individual variations in rete ridges density and depth, collagen fibre organization within the lamina propria and elastin fibre content have been shown to exist in previous histological analyses in humans (Ciano & Beatty, 2015; Couso-Queiruga et al., 2022). Additionally, mapping of these genes within the lamina propria to assess their distribution in the soft tissues would add more information to the biological properties based on location. This knowledge could improve the biological understanding of oral wound healing and, in extension, the nature of soft tissue attachment to the dental surface or adhesion to the dental implant transmucosal components after soft tissue augmentation procedures. These intra-individual and inter-individual variations should be explored in future studies, as they could be applicable when developing personalized treatment plans and subsequent evaluation of long-term outcomes and graft stability.

1600051x, 2023, 10, Downloaded from https://onlinelibrary.wiley.com/doi/10.1111/jcpe.13843 by Schweizerische Akademie Der, Wiley Online Library on [16/09/2023]. See the Terms and Conditions (https://onlinelibrary.wiley.com/terms-and-conditions) on Wiley Online Library for rules of use; OA articles are governed by the applicable Creative Commons License

5 | CONCLUSIONS

Oral mucosa samples harvested from various intra-oral locations (AP, PP, MT and RP) were found to be structurally and genetically distinct. MT and RP samples exhibited more heterogeneity, whereas AP and PP samples shared a similar genetic profile. Genes involved in collagen maturation and extracellular matrix regulation were overexpressed in MT and RP samples, while genes related to lipogenesis were markedly expressed in the palatal region. The biological behaviour and long-term therapeutic outcomes of soft tissue augmentation procedures may be influenced by the biological profile of the intra-oral donor site.

AUTHOR CONTRIBUTIONS

Sandra Stuhr, Emilio Couso-Queiruga, Gustavo Avila-Ortiz and Sukirth M. Ganesan contributed to the conception, design, data acquisition and interpretation of data. Sandra Stuhr completed all tissue sectioning, and Sandra Stuhr and Kareem Gayar performed the collagen staining. Gustavo Avila-Ortiz captured the photomicrographs. Sandra Stuhr and Felipe Nör completed the quantitative measurements and data analysis. Felipe Nör led the histological analysis. Sukirth M. Ganesan performed the statistical analysis, gene expression profiles and real time polymerase chain reaction (qPCR) analysis. Sandra Stuhr and Gustavo Avila-Ortiz created the figures and illustrations. Sandra Stuhr, Emilio Couso-Queiruga and Sukirth M. Ganesan led the writing. Felipe Nör, Leandro Chambrone, Iñaki Gamborena, Purnima Kumar and Gustavo Avila-Ortiz critically revised the manuscript. All authors gave final approval and agreed to be accountable for all aspects of the scientific work.

ACKNOWLEDGEMENTS

This study was supported by the Phillip A. Lainson Professorship in Periodontics at the University of Iowa College of Dentistry and Dental Clinics. We would like to thank Ms. Kaitlin Wenndt, Department of Oral Pathology, Radiology and Medicine, College of Dentistry, University of Iowa, for her expertise and technical support during the study. We would also like to thank Dr. Christopher Hogden, Department of Endodontics, College of Dentistry, University of Iowa, for his valuable assistance in the laboratory.

CONFLICT OF INTEREST STATEMENT

The authors have no conflicts of interest pertaining to this study.

DATA AVAILABILITY STATEMENT

The data that support the findings of this study are available from the corresponding author upon reasonable request.

ORCID

Leandro Chambrone https://orcid.org/0000-0002-2838-1015

REFERENCES

Avila-Ortiz, G., Couso-Queiruga, E., Pirc, M., Chambrone, L., & Thoma, D. S. (2022). Outcome measures and methods of assessment of soft-tissue augmentation interventions in the context of dental implant therapy: A systematic review of clinical studies published in the last 10 years. *Clinical Oral Implants Research*, *34*(Suppl 25), 84–96. https://doi.org/10.1111/clr.13927

Barootchi, S., Tavelli, L., Zucchelli, G., Giannobile, W. V., & Wang, H. L. (2020). Gingival phenotype modification therapies on natural teeth: A network meta-analysis. *Journal of Periodontology*, *91*(11), 1386–1399. https://doi.org/10.1002/JPER.19-0715

Bertl, K., Pifl, M., Hirtler, L., Rendl, B., Nürnberger, S., Stavropoulos, A., & Ulm, C. (2015). Relative composition of fibrous connective and fatty/-glandular tissue in connective tissue grafts depends on the harvesting technique but not the donor site of the hard palate. *Journal of periodontology*, *86*(12), 1331–1339. https://doi.org/10.1902/jop.2015.150346

Byrd, K. M., Piehl, N. C., Patel, J. H., Huh, W. J., Sequeira, I., Lough, K. J., Wagner, B. L., Marangoni, P., Watt, F. M., Klein, O. D., Coffey, R. J., & Williams, S. E. (2019). Heterogeneity within stratified epithelial stem cell populations maintains the oral mucosa in response to physiological stress. *Cell Stem Cell*, *25*(6), 814–829 e816. https://doi.org/10.1016/j.stem.2019.11.005

Cairo, F., Nieri, M., & Pagliaro, U. (2014). Efficacy of periodontal plastic surgery procedures in the treatment of localized facial gingival recessions. A systematic review. *Journal of Clinical Periodontology*, *41*(Suppl 15), S44–S62. https://doi.org/10.1111/jcpe.12182

Chambrone, L., Chambrone, D., Pustiglioni, F. E., Chambrone, L. A., & Lima, L. A. (2008). Can subepithelial connective tissue grafts be considered the gold standard procedure in the treatment of Miller Class I and II recession-type defects? *Journal of Dentistry*, *36*(9), 659–671. https://doi.org/10.1016/j.jdent.2008.05.007

Chambrone, L., & Ortiz, G. A. (2022). *Tissues: Critical issues in periodontal and implant-related plastic and reconstructive surgery*. Quintessence Publishing.

Chambrone, L., Salinas Ortega, M. A., Sukekava, F., Rotundo, R., Kalemaj, Z., Buti, J., & Pini Prato, G. P. (2018). Root coverage procedures for treating localised and multiple recession-type defects. *Cochrane Database of Systematic Reviews*, *10*, CD007161. https://doi.org/10.1002/14651858.CD007161.pub3

Ciano, J., & Beatty, B. L. (2015). Regional quantitative histological variations in human oral mucosa. *The Anatomical Record*, *298*(3), 562–578. https://doi.org/10.1002/ar.23097

Collins, J. M., Neville, M. J., Pinnick, K. E., Hodson, L., Ruyter, B., van Dijk, T. H., Reijngoud, D. J., Fielding, M. D., & Frayn, K. N. (2011). De novo lipogenesis in the differentiating human adipocyte can provide all fatty acids necessary for maturation. *Journal of Lipid Research*, *52*(9), 1683–1692. https://doi.org/10.1194/jlr.M012195

Couso-Queiruga, E., Gonzalez-Martin, O., Stuhr, S., Gamborena, I., Chambrone, L., & Avila-Ortiz, G. (2022). Comparative histological evaluation of intra- and extraorally de-epithelialized connective tissue graft samples harvested from the posterior palate region. *Journal of Periodontology*, *94*, 652–660. https://doi.org/10.1002/JPER.22-0493

Del Pizzo, M., Modica, F., Bethaz, N., Priotto, P., & Romagnoli, R. (2002). The connective tissue graft: A comparative clinical evaluation of wound healing at the palatal donor site. A preliminary study. *Journal of Clinical Periodontology*, *29*(9), 848–854. https://doi.org/10.1034/j.1600-051x.2002.290910.x

Dellavia, C., Ricci, G., Pettinari, L., Allievi, C., Grizzi, F., & Gagliano, N. (2014). Human palatal and tuberosity mucosa as donor sites for ridge augmentation. *The International Journal of Periodontics & Restorative Dentistry*, *34*(2), 179–186. https://doi.org/10.11607/prd.1929

Gamborena, I. B., & Markus, B. (2014). *Evolution: Contemporary protocols for anterior single-tooth implants*. Quintessence Publishing.

Gluckman, H., Du Toit, J., Pontes, C. C., & Hille, J. (2019). Hyperplastic response following soft tissue augmentation in the esthetic zone. *Clinical Advances in Periodontics*, *9*(2), 50–54. https://doi.org/10.1002/cap.10047

1600051x, 2023, 10, Downloaded from https://onlinelibrary.wiley.com/doi/10.1111/jcpe.13843 by Schweizerische Akademie Der, Wiley Online Library on [16/09/2023]. See the Terms and Conditions (https://onlinelibrary.wiley.com/terms-and-conditions) on Wiley Online Library for rules of use; OA articles are governed by the applicable Creative Commons License

Griffin, T. J., Cheung, W. S., Zavras, A. I., & Damoulis, P. D. (2006). Postoperative complications following gingival augmentation procedures. *Journal of Periodontology*, *77*(12), 2070–2079. https://doi.org/10.1902/jop.2006.050296

Harris, R. J. (2003). Histologic evaluation of connective tissue grafts in humans. *The International Journal of Periodontics & Restorative Dentistry*, *23*(6), 575–583 https://www.ncbi.nlm.nih.gov/pubmed/14703761

Jung, U. W., Um, Y. J., & Choi, S. H. (2008). Histologic observation of soft tissue acquired from maxillary tuberosity area for root coverage. *Journal of Periodontology*, *79*(5), 934–940. https://doi.org/10.1902/jop.2008.070445

Kagan, H. (1986). *Regulation of matrix accumulation* (Vol. 1). Academic Press.

Kamel, M., Wagih, M., Kilic, G. S., Diaz-Arrastia, C. R., Baraka, M. A., & Salama, S. A. (2017). Overhydroxylation of lysine of collagen increases uterine fibroids proliferation: Roles of lysyl hydroxylases, lysyl oxidases, and matrix metalloproteinases. *BioMed Research International*, *2017*, 5316845. https://doi.org/10.1155/2017/5316845

Liu, J., & Hoh, J. (2017). Loss of complement factor H in plasma increases endothelial cell migration. *Journal of Cancer*, *8*(12), 2184–2190. https://doi.org/10.7150/jca.19452

Liu, W., Zhang, T., Guo, L., Wang, Y., & Yang, Y. (2018). Lysyl hydroxylases are transcription targets for GATA3 driving lung cancer cell metastasis. *Scientific Reports*, *8*(1), 11905. https://doi.org/10.1038/s41598-018-30309-9

Meltzer, J. A. (1979). Edentulous area tissue graft correction of an esthetic defect. A case report. *Journal of Periodontology*, *50*(6), 320–322. https://doi.org/10.1902/jop.1979.50.6.320

Perrier, S., Kherratia, B., Deschaumes, C., Ughetto, S., Kemeny, J. L., Baudet-Pommel, M., & Sauvezie, B. (2002). IL-1ra and IL-1 production in human oral mucosal epithelial cells in culture: Differential modulation by TGF-beta1 and IL-4. *Clinical and Experimental Immunology*, *127*(1), 53–59. https://doi.org/10.1046/j.1365-2249.2002.01685.x

Sanz-Martin, I., Rojo, E., Maldonado, E., Stroppa, G., Nart, J., & Sanz, M. (2019). Structural and histological differences between connective tissue grafts harvested from the lateral palatal mucosa or from the tuberosity area. *Clinical Oral Investigations*, *23*(2), 957–964. https://doi.org/10.1007/s00784-018-2516-9

Smith, J. M., Johanesen, P. A., Wendt, M. K., Binion, D. G., & Dwinell, M. B. (2005). CXCL12 activation of CXCR4 regulates mucosal host defense through stimulation of epithelial cell migration and promotion of intestinal barrier integrity. *American Journal of Physiology. Gastrointestinal and Liver Physiology*, *288*(2), G316–G326. https://doi.org/10.1152/ajpgi.00208.2004

Tavelli, L., Barootchi, S., Avila-Ortiz, G., Urban, I. A., Giannobile, W. V., & Wang, H. L. (2021). Peri-implant soft tissue phenotype modification and its impact on peri-implant health: A systematic review and network meta-analysis. *Journal of Periodontology*, *92*(1), 21–44. https://doi.org/10.1002/JPER.19-0716

Tavelli, L., Barootchi, S., Greenwell, H., & Wang, H. L. (2019). Is a soft tissue graft harvested from the maxillary tuberosity the approach of choice in an isolated site? *Journal of Periodontology*, *90*(8), 821–825. https://doi.org/10.1002/JPER.18-0615

van der Slot, A. J., Zuurmond, A. M., van den Bogaerdt, A. J., Ulrich, M. M., Middelkoop, E., Boers, W., Karel Ronday, H., DeGroot, J., Huizinga, T. W., & Bank, R. A. (2004). Increased formation of pyridinoline cross-links due to higher telopeptide lysyl hydroxylase levels is a general fibrotic phenomenon. *Matrix Biology*, *23*(4), 251–257. https://doi.org/10.1016/j.matbio.2004.06.001

von Elm, E., Altman, D. G., Egger, M., Pocock, S. J., Gotzsche, P. C., Vandenbroucke, J. P., & Initiative, S. (2007). Strengthening the Reporting of Observational Studies in Epidemiology (STROBE) statement: Guidelines for reporting observational studies. *BMJ*, *335*(7624), 806–808. https://doi.org/10.1136/bmj.39335.541782.AD

Walker, L. C., Overstreet, M. A., & Yeowell, H. N. (2005). Tissue-specific expression and regulation of the alternatively-spliced forms of lysyl hydroxylase 2 (LH2) in human kidney cells and skin fibroblasts. *Matrix Biology*, *23*(8), 515–523. https://doi.org/10.1016/j.matbio.2004.11.002

Wang, A., Fairhurst, A. M., Tus, K., Subramanian, S., Liu, Y., Lin, F., Igarashi, P., Zhou, X. J., Batteux, F., Wong, D., Wakeland, E. K., & Mohan, C. (2009). CXCR4/CXCL12 hyperexpression plays a pivotal role in the pathogenesis of lupus. *Journal of Immunology*, *182*(7), 4448–4458. https://doi.org/10.4049/jimmunol.0801920

Xia, J., Chen, N., Hong, Y., Chen, X., Tao, X., Cheng, B., & Huang, Y. (2012). Expressions of CXCL12/CXCR4 in oral premalignant and malignant lesions. *Mediators of Inflammation*, *2012*, 516395. https://doi.org/10.1155/2012/516395

Yang, M., Song, L., Wang, L., Yukht, A., Ruther, H., Li, F., Qin, M., Ghiasi, H., Sharifi, B. G., & Shah, P. K. (2018). Deficiency of GATA3-positive macrophages improves cardiac function following myocardial infarction or pressure overload hypertrophy. *Journal of the American College of Cardiology*, *72*(8), 885–904. https://doi.org/10.1016/j.jacc.2018.05.061

Zito, E., Hansen, H. G., Yeo, G. S., Fujii, J., & Ron, D. (2012). Endoplasmic reticulum thiol oxidase deficiency leads to ascorbic acid depletion and noncanonical scurvy in mice. *Molecular Cell*, *48*(1), 39–51. https://doi.org/10.1016/j.molcel.2012.08.010

Zuhr, O., Baumer, D., & Hurzeler, M. (2014). The addition of soft tissue replacement grafts in plastic periodontal and implant surgery: Critical elements in design and execution. *Journal of Clinical Periodontology*, *41*(Suppl 15), S123–S142. https://doi.org/10.1111/jcpe.12185

SUPPORTING INFORMATION

Additional supporting information can be found online in the Supporting Information section at the end of this article.

How to cite this article: Stuhr, S., Nör, F., Gayar, K., Couso-Queiruga, E., Chambrone, L., Gamborena, I., Kumar, P., Avila-Ortiz, G., & Ganesan, S. M. (2023). Histological assessment and gene expression analysis of intra-oral soft tissue graft donor sites. *Journal of Clinical Periodontology*, *50*(10), 1360–1370. https://doi.org/10.1111/jcpe.13843

1600051x, 2023, 10, Downloaded from https://onlinelibrary.wiley.com/doi/10.1111/jcpe.13843 by Schweizerische Akademie Der, Wiley Online Library on [16/09/2023]. See the Terms and Conditions (https://onlinelibrary.wiley.com/terms-and-conditions) on Wiley Online Library for rules of use; OA articles are governed by the applicable Creative Commons License